Observations of Photoelectron Energy Peaks Below 400 km in the Dayside Ionosphere of Mars

Frahm, R. A., J. D. Winningham, J. R. Sharber, S. J. Jeffers, (Southwest Research Institute, San Antonio, TX 78228, USA),
A. J. Coates, D. R. Linder, (Mullard Space Science Laboratory, University College London, United Kingdom)
and ASPERA-3* Team (Swedish Institute of Space Physics, Box 812 S-981 28, Kiruna, Sweden)

ABSTRACT

The Mars Express Analyzer of Space Plasmas and Energetic Atoms (ASPERA-3) experiment determines the electron, ion, and neutral particle components of plasma using four instruments: Electron Spectrometer (ELS), Ion Mass Analyzer (IMA), Neutral Particle Imager (NPI), and Neutral Particle Detector (NPD). The ELS instrument determines the electron energy spectrum by collecting 128 logarithmically spaced samples of the electron spectrum between 1 eV and 20 keV every four seconds. When the ASPERA-3 makes measurements within the dayside Martian ionosphere, it detects electrons from the 30.4 nm photoionization peaks of carbon dioxide and atomic oxygen. These photoelectron peaks are typically observed in all ELS directional sectors when they are detected. Thus, spectrograms in the ionosphere have been examined for one ELS sector in a pilot study to determine if and where the electron photoelectron peaks are observed with respect to the planet surface. The locations of these peaks are compared to the map of the radial component of the crustal magnetic fields to determine if the crustal magnetic fields influence the locations of photoelectrons. The comparison is restricted to the region below an altitude of 400 km and bounded at low altitudes by the spacecraft periapsis (250-300 km).

INTRODUCTION

In December of 2003, the Mars Express (MEX) spacecraft reached Mars carrying the Analyzer of Space Plasmas and Energetic Atoms experiment (ASPERA-3) [Barabash *et al.*, 2004]. This plasma experiment contained an Electron Spectrometer (ELS) along with ion and neutral particle detectors. The ELS observed photoelectron energy peaks at low altitudes near Mars as well as at distant locations in the Martian tail [Frahm *et al.*, 2006a]. These photoelectron peaks were shown by both Mantas and Hanson [1979] and Fox and Delgarno [1979] to be a significant feature at Mars. Mantas and Hanson also described the photoelectron spectrum under two different magnetic field orientations, vertical and horizontal magnetic field. The vertical magnetic field provided a description of the electron spectrum for the condition of direct atmospheric escape of electrons, whereas the horizontal magnetic field provided a description of the electron spectrum for which the magnetic field acted as a restraining barrier to the vertical transport of electrons. This study is an attempt to discover from where the photoelectrons in the tail of Mars come.

ELS measurements of the photoelectron spectrum made when the MEX spacecraft was below 400 km at Mars indicated that the photoelectron energy peaks observed were observed simultaneously in all ELS sectors, which was not the case at higher altitudes. Larger altitude measurements tended to emphasize the flow of electrons and their signature is observed to be sector dependent at larger altitudes. For this investigation, we will restrict observations to altitudes less than 400 km where the photoelectron energy peak signature is observed in all ELS sectors. We are interested to discover if there is any preference in the location at which photoelectron peaks near Mars are observed. **In particular, are the locations of the photoelectron peaks measured by ELS related to the position of the crustal magnetic fields which were measured by the Mars Global Surveyor (MGS) magnetometer [Connerney et al, 2001].**

INSTRUMENT

The ELS is a spherical top-hat analyzer with a 360° field of view in the measurement plane and 4°. width in elevation. The 360° measurement plane is divided into 16 sectors, each sector was 22.5° wide. The ELS analyzer constant and energy resolution are slightly sector dependent, averaging 7.23 ± 0.05 eV/volt and 0.083 ± 0.003 eV/eV respectively. The energy independent geometric factor is 5.88×10^{-4} cm² sr.

The ELS energy range is covered by using a linear dual-range power supply which covers up to about 150 eV in low range and up to about 20 keV in high range. In general, the energy range of ELS covered from 0.4 eV to 20 keV logarithmically in 127 out of a possible 8192 energy steps (1 step has been discarded due to flyback) within 4 sec (its main configuration). The secondary configuration covered and energy range from 1 eV to 127 eV (linearly stepped every eV) in 4 sec. Additional ELS configurations were used sparingly.

The ELS contains a grid placed between the energy analyzer and its microchannel plate detector. The purpose of this grid is to protect the detector by repelling low-energy electrons so that they do not reach the detector. The protection grid voltage has varied as the instrument has aged. Initially, the protection grid was set to -5V, repelling electrons below 5 eV from entering the detector. At various times, the protection grid voltage has been set to values between -5V and 0V.

DATA

All data used in this paper has been generated from a pilot study data conducted using flux measurements from ELS sector 3 only, between January 5, 2004 and January 5, 2005. The pilot study contained ELS data irrespective of ELS mode. The ELS mode varied between various high, medium, and low energy resolution modes, and medium to low time resolution modes [Frahm *et al.*, 2006b]. The ELS energy was stepped both logarithmicly and linearly over the measurement range.

Data from spectrograms were analyzed to determine the locations of the photoelectron energy peaks. Survey plots were examined as shown in Figure 1a. These data are viewed in standard energy versus time spectrograms of the energy flux showing two panels covering different energy ranges and having different color scales of energy flux. The top panel shows the full ELS energy range using a 4 decade color scale revealing the overall context of the ELS data. Overlaid is the integral intensity between 5 eV and 100 eV. The lower panel shows a blow-up of the energy region below 100 eV. A smaller range of the energy flux color scale is used to highlight the photoelectron energy peaks even though the color is often saturated at other features. Overlaid on this panel is the spacecraft altitude. At the bottom of this panel is shown the solar zenith angle.

During the selection process, when a positive identification of photoelectron peaks is made, the time (which translate into positions along the spacecraft track) is recorded. During the pilot study, the photoelectron peaks were observed to disappear as in Figure 1a from 1 January 2005 between 00:35:30 UT and 00:38:30 UT, or to become obscured as in Figure 2a from 3 January 2005 between 06:30:30 UT and 06:33:30 UT.

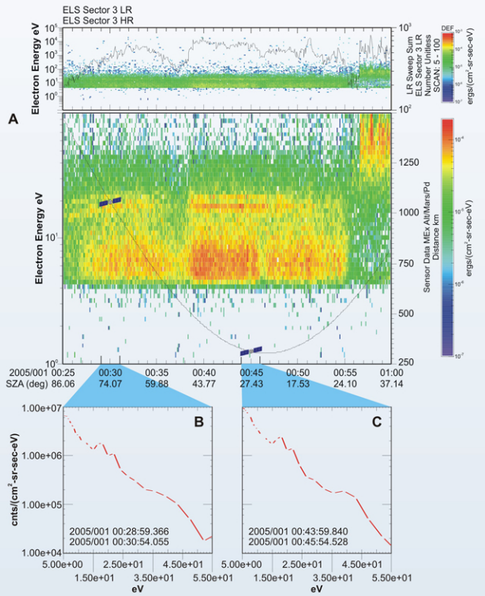

Figure 1. Dropout Example in Photoelectron Peaks. Energy-time spectrograms of the electron energy flux for the full range and photoelectron region are shown in (A) for 1 January 2005. There is a dropout in the photoelectron peaks observed between 00:35:30 UT and 00:38:30 UT. The electron spectra both before (B) and after (C) the dropout are presented to show photoelectron peaks on each side of the dropout.

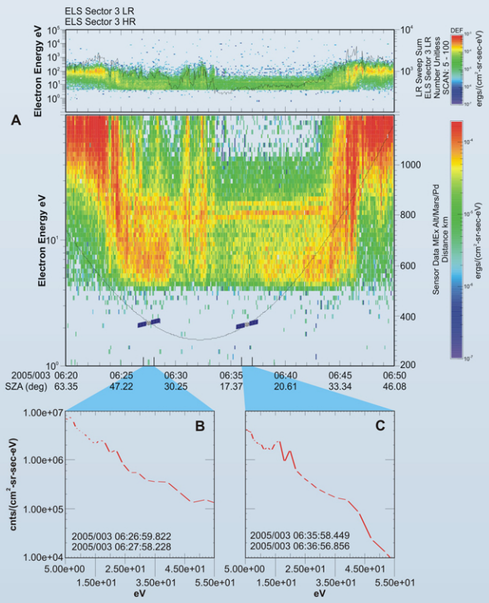

Figure 2. Obscured Photoelectron Peaks Example. Energy-time spectrograms of the electron energy flux for the full range and photoelectron region are shown in (A) for 3 January 2005. The photoelectron peaks are observed to be obscured between 06:30:30 UT and 06:33:30 UT. The electron spectrum both before (B) and after (C) the photoelectron peaks are obscured are presented to show that they are observed on each side of the obscuring fluxes.

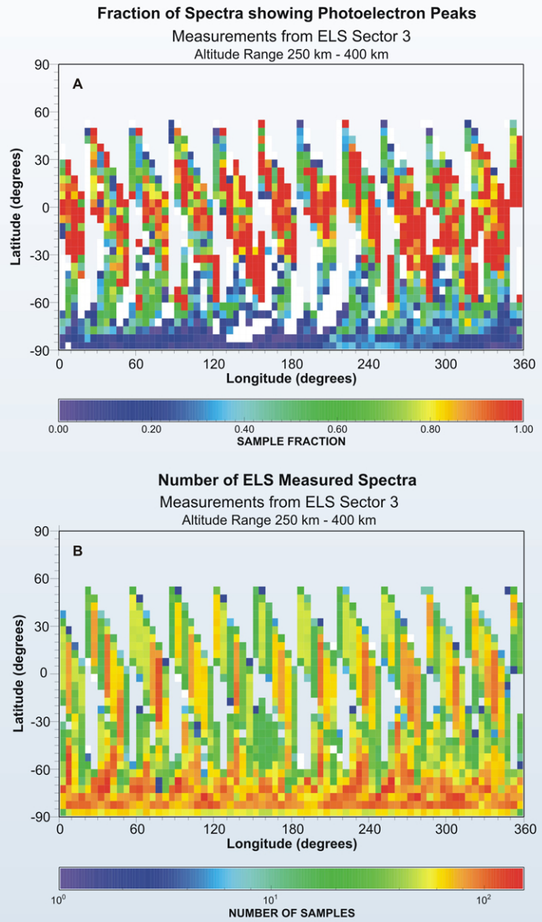

Figure 3. Observed location of Photoelectron Peaks. Shown are locations where ELS measured photoelectron peaks in (A) as a fraction of the amount of times ELS sampled. The number of times ELS sampled are shown in (B). The planetodetic grid is 5° in latitude and 5° in longitude.

RESULTS

Data from the pilot study was mapped into the frame of the planet with a grid resolution of 5° in latitude, 5° in longitude, and 10 km in altitude. For this study, the altitudes below 400 km were collected and presented together as Figure 3. Figure 3a shows the locations where photoelectron peaks are observed while locations where the spacecraft made measurements are shown in Figure 3b. During this time period, the spacecraft periapsis began at 250 km, but gradually increased to 300 km over the study time frame.

Observable in Figure 3b are locations of the planetodetic system which are not measured (Mars Radius = 3393 km) by the ELS. These locations are shown as the background color. During this time frame, no measurements were made above 55° latitude when the spacecraft was below 400 km altitude. The vertical striping at mid-latitudes reflects the motion of the spacecraft near perigee, where the rotation of the planet is insignificant to the motion in latitude of the spacecraft. Also reflected in Figure 3a are the locations where no photoelectron peaks were measured. Comparison between Figure 3a and 3b shows that the fractional occurrence of photoelectrons occurs least near the southern hemisphere pole; however, there is a location of reduced fraction of photoelectrons observed between 160° to 240° longitude and -30° latitude to the southern pole. This pattern will become more clear as additional data are added to the pilot study.

DISCUSSION

The pattern of photoelectrons looks suspiciously related to the location where the intense radial component was reported by the Mars Global Surveyor Magnetometer. Figure 4 shows the published locations of radial component of the magnetic anomalies at 400 km [Connerney *et al.*, 2001]. Strikingly the anomalies are stronger and more numerous in the southern highlands, the same region that was pointed out in Figure 3, between 160° to 240° longitude and -30° latitude to the southern pole.

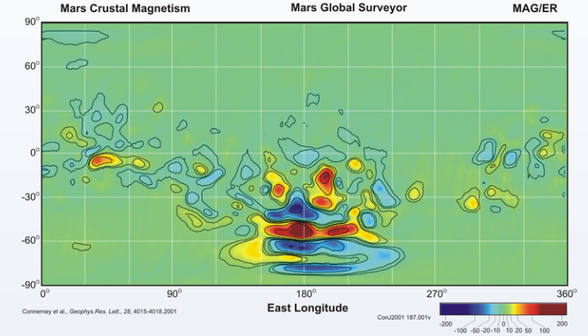

Figure 4. Radial Magnetic Field at 400 km. Shown are contours of the radial component of the radial magnetic field on Mars as measured by the MGS magnetometer and described by Connerney et al., 2001.

Despite the lack of anomaly field about the southern magnetic pole, the lack of photoelectron observations could be a due to high solar zenith angle, where theory has shown fewer photoelectrons are produced. This should not be true in mid-latitudes where the effect of the solar zenith angle is minor.

At locations where the radial magnetic field is weak or non-existent, photoelectrons may be traveling on closed field lines and form a trapped population. This situation is similar to that of the horizontal magnetic field shown by Mantas and Hanson [1979]. Here, Mantas and Hanson showed that within the confines of their model, photoelectron intensities build until their destruction mechanisms balance their creation mechanism. However, in the case of the anomaly field, the component of the radial field provides a means whereby the photoelectrons created at lower altitudes can escape to higher altitudes. This reflects the vertical field case shown by Mantas and Hanson. Here the model photoelectron intensities can be lower because flux escapes along the magnetic field before being destroyed in the atmosphere.

So we are left with seemingly conflicting information. One suspects that the radial component of the magnetic field channels the photoelectrons into the deep tail; however, lower occurrences of photoelectrons are observed when the radial anomaly field is strongest.

CONCLUSION

A pilot study of the location of observation of ELS photoelectron peaks was presented for altitudes below 400 km with the following results:

- The majority of observed photoelectron peaks occurred at mid-latitudes.
- Within this mid-latitude band is a region of reduced occurrence rate of the photoelectron peaks, which appears to correlate with the regions of largest intensity of the radial component of the magnetic field as measured by the MGS magnetometer.
- Lower occurrence rates of photoelectron peaks were found in the region around the southern hemisphere pole.

There was no data acquired within the limits (time and altitude) of this study at latitudes greater than 55 degrees.

REFERENCES

Barabash, S., R. Lundin, H. Andersson, J. Gimholt, M. Holmstrom, O. Norberg, M. Yamauchi, K. Asamura, A. J. Coates, D. R. Linder, D. O. Kataria, C. C. Curtis, K. C. Hsieh, B. R. Sandel, A. Fedorov, A. Grigoriev, E. Budnik, M. Grande, M. Carter, D. H. Reading, H. Koskinen, E. Kallio, P. Riihela, T. Sales, J. Kozyra, N. Krupp, S. Livi, J. Woch, J. Luhmann, S. McKenna-Lawlor, S. Orsini, R. Cerulli-Irelli, A. Mura, A. Milillo, E. Roelof, D. Williams, J.-A. Sauvaud, J.-J. Thocaven, D. Winningham, R. Frahm, J. Scherrer, J. Sharber, P. Wurz, and P. Bochsler, "ASPERA-3: Analyser of Space Plasmas and Energetic Ions for the Mars Express," in Mars Express: The Scientific Payload, eds. A. Wilson and A. Chicarro, European Space Agency special report SP-1240, European Space Agency Research and Scientific Support, European Space Research and Technology Centre, Noordwijk, The Netherlands, 121-139, August 2004.

Connerney, J. E. P., M. H. Acuna, P. J. Wasilewski, G. Kletetschka, N. F. Ness, H. Reme, R. P. Lin, and D. L. Mitchell, "The Global Magnetic Field of Mars and Implications for Crustal Evolution," Geophysical Research Letters, Vol. 28, 4015-4018, 2001.

Fox, J. L., and A. Dalgarno, "Ionization, Luminosity, and Heating of the Upper Atmosphere of Mars," Journal of Geophysical Research, 84, 7315-7333, 1979.

Frahm, R. A., J. D. Winningham, J. R. Sharber, J. R. Scherrer, S. J. Jeffers, A. J. Coates, D. R. Linder, D. O. Kataria, R. Lundin, S. Barabash, M. Holmstrom, H. Andersson, M. Yamauchi, A. Grigoriev, E. Kallio, T. Sales, P. Riihela, W. Schmidt, H. Koskinen, J. U. Kozyra, J. G. Luhmann, E. C. Roelof, D. J. Williams, S. Livi, C. C. Curtis, K. C. Hsieh, B. R. Sandel, M. Grande, M. Carter, J.-A. Sauvaud, A. Fedorov, J.-J. Thocaven, S. McKenna-Lawlor, S. Orsini, R. Cerulli-Irelli, M. Maggi, P. Wurz, P. Bochsler, N. Krupp, J. Woch, M. Franz, K. Asamura, and C. Dierker, "Carbon dioxide photoelectron energy peaks at Mars," Icarus, 182, 371-382, 2006a.

Frahm, R. A., J. R. Sharber, J. D. Winningham, P. Wurz, M. W. Liemohn, E. Kallio, M. Yamauchi, R. Lundin, S. Barabash, A. J. Coates, D. R. Linder, J. U. Kozyra, M. Holmstrom, S. J. Jeffers, H. Andersson, and S. Mckenna-Lawlor, "Locations of Atmospheric Photoelectron Energy Peaks Within the Mars Environment," Space Science Reviews, Volume 126, Numbers 1-4, 389-402, DOI 10.1007/s11214-006-9119-5, October, 2006b.

Mantas, G. P., and W. B. Hanson, "Photoelectron Fluxes in the Martian Ionosphere," Journal of Geophysical Research, 84, 369-385, 1979.

* ASPERA-3 Team

R. A. Frahm, J. D. Winningham, J. R. Sharber, SwRI, San Antonio, USA
A. J. Coates, D. R. Linder, D. O. Kataria, Mullard Space Science Laboratory, UCL, UK
R. Lundin, H. Anderson, S. Barabash, M. Holmström, M. Yamauchi, Swedish Institute of Space Physics, Sweden
E. Kallio, H. Koskinen, Finnish Meteorological Institute, Helsinki, Finland
J. Kozyra, Space Physics Research Laboratory, U. Michigan, Ann Arbor, USA
J. Luhmann, University of California Berkeley, USA
E. Roelof, D. Williams, JHU-APL, Laurel, USA
C.C. Curtis, K. C. Hsieh, B. R. Sandel, University of Arizona, Tucson, USA
J. A. Sauvaud, A. Federov, Centre d'Etude Spatiale des Rayonnements, France
S. McKenna-Lawlor, Space Technology Ltd, Maynooth, Ireland
S. Orsini, R. Cerulli-Irelli, Institute di Fisica dello Spazio Interplantari, Italy
P. Bochsler, P. Wurz, University of Bern, Bern Switzerland
K. Azamura, ISAS, Japan
M. Grande, Institute of Mathematical and Physical Sciences, U. of Wales, Aberystwyth, Ceredigion, Wales, UK
N. Krupp, J. Woch, M. Fraenz, Max-Planck-Institut fur Aeronomie, Germany